

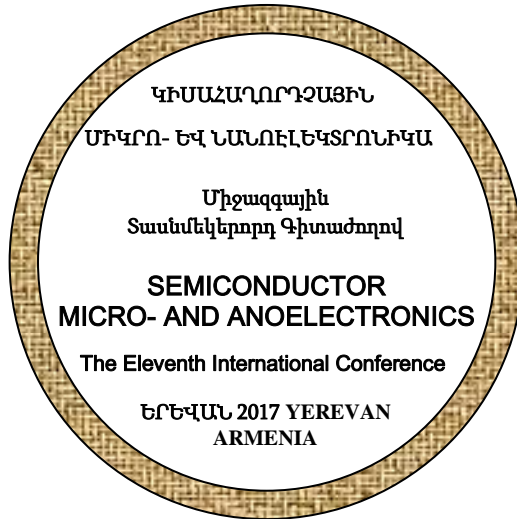
ԵՐԵՎԱՆԻ ՊԵՏԱԿԱՆ ՀԱՄԱԼՍԱՐԱՆ

ՀԱՅԱՍՏԱՆԻ ՀԱՆՐԱՊԵՏՈՒԹՅԱՆ ԳԻՏՈՒԹՅՈՒՆՆԵՐԻ  
ԱԶԳԱՅԻՆ ԱԿԱԴԵՄԻԱ

**ԿԻՍԱՀԱՂՈՐԴՉԱՅԻՆ  
ՄԻԿՐՈ- ԵՎ ՆԱՆՈԷԼԵԿՏՐՈՆՆԻԿԱ**

ՏԱՍՆՍԵԿԵՐՈՐԴ ՄԻԶԱԶԳԱՅԻՆ ԳԻՏԱԺՈՂՈՎԻ ՆՅՈՒԹԵՐ  
ԵՐԵՎԱՆ, 23-25 ՀՈՒՆԻՍ

**SEMICONDUCTOR  
MICRO- AND NANOELECTRONICS  
PROCEEDINGS OF THE ELEVENTH INTERNATIONAL  
CONFERENCE  
YEREVAN, ARMENIA, JUNE 23-25**



**Երևան**

**ԵՊՀ հրատարակչություն**

**2017**

# COMPETING NUCLEATION OF ISLANDS AND NANOPITS IN ZINC-BLEND AND WURTZIT GaN-InN-AIN QUATERNARY MATERIAL SYSTEM

*K.M. Gambaryan, A.K. Simonyan and Y.M. Baghiyan*

*Yerevan State University, Armenia. E-mail: kgambaryan@ysu.am*

## **1. Introduction**

During the last two decades, the use of quantum dots (QDs), corresponding semiconducting materials and their band gap engineering, opens up entirely new functionalities of traditional devices as well as new challenges for the fabrication of devices with unique properties. In particular, single photon sources for quantum cryptography, quantum dot lasers, single photon detectors, single electron transistors, resonant tunneling diodes, etc [1-4]. Indeed, the physical properties of QDs depend on QDs size and shape, as well as on the mechanism of their formation. The most useful approach for the fabrication of QDs is Stranski–Krastanow growth mode, where the sum of the surface free energy and the interface free energy is about the same as the substrate free energy. In this case, the wetting layer is compressively strained in a few percent. Interestingly note that in the original publication by Stranski and Krastanow, no strain effects were considered. The strain relaxation leads to the formation of coherent (dislocation free) islands on top of a thin wetting layer. Depending on the strain value and its sign, the growth of QDs, the formation of nanopits or even QDs–nanopits cooperative structure can be achieved. Binary III-V compound semiconductors, especially nitrides and their ternary and quaternary alloy are very attractive for several applications [5]. For instance, GaInN alloys are used for fabrication of blue and green light emitted diodes, as well as for violet and blue lasers [6]. Since the band gap of GaInN can be varied from 2.0 to 3.5 eV by increasing of GaN concentration, the potential operating wavelengths cover nearly the entire visible spectra range [7, 8]. High-speed field effect transistors, high-temperature electronic devices, UV and blue light emitters, detectors and gas sensors were made of GaN [9]. Among III-nitride semiconductors, InN has lowest effective mass and small band gap. Therefore, InN-related solid solutions can extend the emission or absorption from the UV to near infrared regions. The photovoltaic (PV) and thermo-PV cells were also fabricated using InN [9]. While cubic film/cubic substrate combinations have been analyzed previously, systems involving hexagonally oriented material as either the film or substrate have not been thoroughly investigated to date. Examples of important semiconductor materials that exist in the hexagonal crystal structure include the wide band gap compound semiconductors GaN, SiC and many II–VI semiconductors. These materials are promising candidates for use in optoelectronic applications including visible and ultraviolet emitters, high power–high temperature electronics. The growth of hexagonal materials has been extensively studied experimentally; quantitative calculation of the inherent strain energy has not been fully performed. Furthermore, the effect of the strain energy on the resulting equilibrium has not been addressed. In [13], elastic compliance equations are developed and their relationship to the overall strain energy of a hexagonally oriented film and substrate are presented. These general relations are then applied to the growth of GaN on different substrates. Additionally, the sufficient lattice mismatch between the III-N binary compounds allows growing of nanostructures in Stranski–Krastanow growth mode.

Regarding the research and development of III-nitride QDs, there are three main kinds of formation mechanism for the growth of QDs. First, it has been proposed [14] that nanoscale indium composition fluctuation due to InGaN phase separation or indium segregation results in the formation of indium-rich clusters, which acts as QDs (QDs-like). Hence, QDs-like system acts as an extremely sophisticated quantum capture system, and in QDs, the charge carriers are deeply localized so as to hinder their migration toward nonradiative defects (dislocations). Therefore, high

luminescence efficiency could be expected if the density of QDs is much higher than that of dislocations. Second, it has been shown that nitride QDs can be self-organized using the strain-induced Stranski-Krastanow growth mode [15]. Third, another way to form nitride QDs is to take advantage of surfactants or antisurfactants, which are often used to change the surface free energy of heterostructure interface. However, the self-assembled nitride QDs can be fabricated by molecular-beam epitaxy or by metalorganic chemical vapor deposition [14, 15] without using any antisurfactants. High-density GaN/AlN QDs for deep UV LED with high quantum efficiency [16] have been also successfully grown by molecular beam epitaxy.

In this paper, the growth mechanism of QDs, nanopits and collaborative QDs-nanopits structures in GaN-InN-AlN material system both for zinc-blend and wurtzite configurations is theoretically investigated using the continuum elasticity model proposed by J. Tersoff (IBM) [1, 10].

## 2. Total energy of island-pit structure in GaN-InN-AlN material system

Here, according to [10] we assume that the zinc-blend GaN substrate has only discrete orientations and therefore only one angle can be used. We also assume that islands and pits have a shape as schematically presented in figure 1(a). High-resolution SEM images of the InAsSbP composition pyramidal island and a nanopit [4] grown on InAs(100) substrate are presented in Figures 1(b,c).

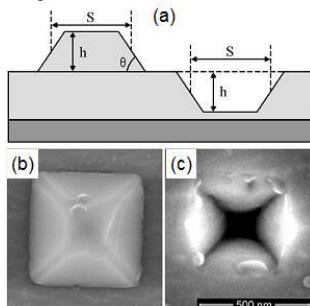


Fig. 1. Schematic view of the island-nanopit structure's cross section – (a), high-resolution SEM images of the InAsSbP composition pyramidal island and a nanopit – (b, c).

As it is known [10], the energy for the formation of an island (or a pit) can be written as  $E = E_s + E_r$ , where  $E_s$  and  $E_r$  are the change in surface energy the reduction of the strain energy by elastic relaxation, respectively. Considering island's volume as a constant, in the case of  $s = t = h \cot \theta$ , where  $s$ ,  $t$ ,  $h$  and  $\theta$  are the length, width, height (depth) and contact angle, as in figure 1(a), the energy is equal to:

$$E = 4\Gamma V^{2/3} T \tan^{1/3} \theta - 6cVT \tan \theta, \quad (1)$$

where  $\Gamma = \gamma_e C s c \theta - \gamma_s C o t \theta$ . For the crystals with a zinc-blend symmetry,  $\gamma_s = \frac{1}{2} \epsilon^2 (C_{11} + C_{44}) d_{wet}$ ,  $c = \sigma_b^2 \frac{(1-\nu)}{2\pi\mu}$ ,  $\sigma_b = \epsilon (C_{11} + C_{44})$ . Here  $\gamma_s$  and  $\gamma_e$  are the surface energy per unit area for the normal orientation and the beveled edge, respectively,  $\epsilon = \frac{\Delta a}{a}$  is the lattice mismatch ratio (strain) and  $d_{wet}$  is the wetting layer thickness. The value for  $\gamma_e$  can be found from Young equation  $\gamma_{sl} = \gamma_s - \gamma_e C o s \theta$  [11], where for Stranski-Krastanow growth mode  $\gamma_{sl} = 0$  is the surface energy corresponding to the solid-liquid interface,  $\nu = \frac{\lambda}{2(\lambda + \mu)}$  is the Poisson ratio,  $\lambda$ ,  $\mu$  and  $C_{ij}$  are the Lamé coefficients and the elastic modulus of the substrate. Finally, the expression for the total energy for the crystals with a zinc-blend and a wurtzite symmetry, respectively, can be written as:  $E = 4 \left( \gamma_e C s c \theta - \frac{1}{2} \epsilon^2 (C_{11} + C_{44}) d_{wet}(\epsilon) C o t \theta \right) V^{2/3} T \tan^{1/3} \theta - 3\epsilon^2 (C_{11} + C_{44})^2 \frac{(1-\nu)}{\pi\mu} V T \tan \theta$ , (2)

$$E = 4 \left( \gamma_e C_{sc} \theta - \frac{1}{S_{11} + S_{12}} \epsilon^2 d_{wet}(\epsilon) \cot \theta \right) V^{2/3} \tan^{1/3} \theta - 3\epsilon^2 \left( \frac{S_{11} - S_{12}}{S_{11}^2 - S_{12}^2} \right)^2 \frac{(1-\nu)}{\pi\mu} V \tan \theta, \quad (3)$$

$$\text{where } S_{11} = \frac{(C_{11}C_{33} - C_{13}^2)}{(C_{11} - C_{12})(C_{11}C_{33} + C_{12}C_{33} - 2C_{13}^2)}, \quad S_{12} = \frac{(C_{13}^2 - C_{12}C_{33})}{(C_{11} - C_{12})(C_{11}C_{33} + C_{12}C_{33} - 2C_{13}^2)} \quad [13].$$

Next, we performed a mathematical approximation of experimental data [12] in order to evaluate for the GaInAlN material system an analytical expression for the dependence of wetting layer thickness versus strain. In our calculations we used the following expressions for  $d_{wet}$  in monolayers (ML): (i) if the deformation strain is positive, then  $d_{wet} = 0.05\epsilon^{-3/2}$  at  $\epsilon > 0.03$  [12] and  $d_{wet} = 24.184e^{-31.034\epsilon}$  at  $0 < \epsilon < 0.03$  (accuracy of approximation  $R^2 = 0.9635$ ), (ii) if the deformation strain is negative, then  $d_{wet} = 0.15|\epsilon|^{-3/2}$  at  $|\epsilon| > 0.035$  [12], and  $d_{wet} = 45.162e^{-23.034|\epsilon|}$  at  $0 < |\epsilon| < 0.035$  (accuracy of approximation  $R^2 = 0.9934$ ).

The results of theoretical calculations of the dependence of GaInAlN composition islands energy on volume at different strains for zinc-blend and wurtzite symmetry, calculated at  $\gamma_e = 10.15 \times 10^{-5} \text{ J/cm}^2$ ,  $\mu = 30.34 \times 10^4 \text{ J/cm}^3$ ,  $C_{11} = 272.3 \times 10^3 \text{ J/cm}^3$ ,  $C_{44} = 130.3 \times 10^3 \text{ J/cm}^3$ ,  $\nu = 0.361$  and  $\theta = 0.785 (45^\circ)$  and  $\gamma_e = 2 \times 10^{-5} \text{ J/cm}^2$ ,  $\mu = 106 \times 10^4 \text{ J/cm}^3$ ,  $C_{11} = 296 \times 10^3 \text{ J/cm}^3$ ,  $C_{12} = 130.3 \times 10^3 \text{ J/cm}^3$ ,  $C_{13} = 158 \times 10^3 \text{ J/cm}^3$ ,  $C_{33} = 267 \times 10^3 \text{ J/cm}^3$ ,  $C_{44} = 241 \times 10^3 \text{ J/cm}^3$ ,  $\nu = 0.37$ ,  $\theta = 0.785 (45^\circ)$  are presented in Figure 2(a, b) and figure 3 (combined), respectively. The dependence of islands critical volume versus strain for the zinc-blend and wurtzite symmetry are presented in figure 4(a, b), respectively.

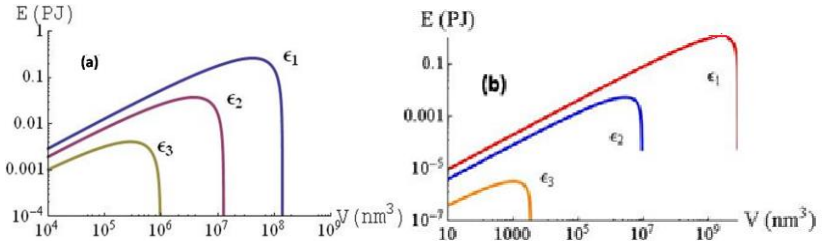


Fig. 2. Dependence of the GaInAlN composition islands energy on volume at different strain for zinc-blend and wurtzite symmetry at different strain ( $\epsilon_1 = 0.02$ ,  $\epsilon_2 = 0.025$ ,  $\epsilon_3 = 0.03$  and  $\epsilon_1 = 0.004$ ,  $\epsilon_2 = 0.008$ ,  $\epsilon_3 = 0.01$ ), respectively.

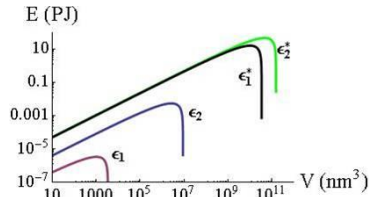


Fig. 3. Dependence of the GaInAlN composition islands energy on volume at different strain for zinc-blend and wurtzite symmetry at  $\epsilon_1 = \epsilon_1^* = 0.008$ ,  $\epsilon_2 = \epsilon_2^* = 0.01$ .

As it can be seen from figures 2 and 3, in order to attain a stable geometry the island must first overcome the energy barrier  $E^*$  which occurs at volume  $V^*$ . It is also quite visible that both  $E^*$  and  $V^*$  strongly depend on the strain and dramatically decrease at the increasing of the strain. At the critical strain of  $\epsilon^* = 0.039$  for zinc-blend and  $\epsilon^* = 0.01$  for wurtzite symmetry, the sign of critical volume (Fig. 4) is changed. We assume that at  $\epsilon = \epsilon^*$  the mechanism of the nucleation is changed from the growth of dots to the nucleation of pits. Clearly, at small misfit ( $\epsilon < \epsilon^*$ ), the bulk

nucleation mechanism dominates. However, at  $\varepsilon > \varepsilon^*$ , when the energy barrier becomes negative as well as a larger misfit provides a low-barrier path for the formation of dislocations, the nucleation of pits becomes energetically preferable. The results of theoretical calculations also show that the critical strain for the wurtzite symmetry is at least three times smaller than that for zinc-blend symmetry.

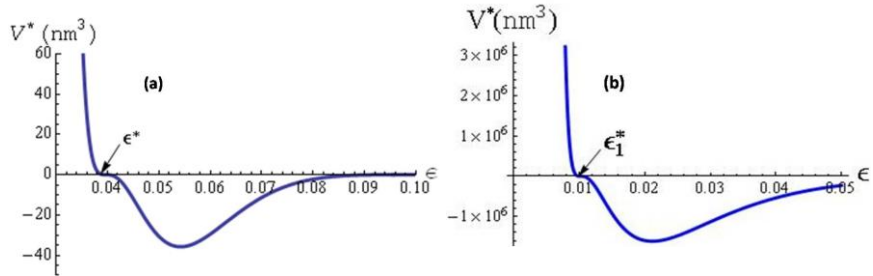


Fig.4. Dependence of the GaInAlN composition islands critical volume versus strain for zinc-blend and wurtzite symmetry, respectively.

### 3. Conclusion

Thus, the growth mechanism of quantum dots (QDs), nanopits and collaborative QDs-nanopits structures in GaN-InN-AlN material system is theoretically investigated using the continuum elasticity model. The islands energy versus their volume, as well as the critical energy and volume versus the island and wetting layer lattice constants relative mismatch ratio (strain  $\varepsilon$ ), are calculated. It was shown that when the zinc-blend GaN is used as a substrate and when the strain between the wetting layer and a substrate overcomes critical  $\varepsilon^* = 0.039$  value, instead of QDs nucleation, the formation of nanopits becomes energetically preferable. Otherwise, when wurtzite GaN is used as a substrate the critical strain is equal to  $\varepsilon^* = 0.01$ , i.e. at least three times smaller. Revealed features have to be taking into account not only at QDs engineering, but also at the growth of bulk crystals and epitaxial thin films in GaInAlN material system.

### References

1. J. Tersoff and F.K. Le Goues. Phys. Rev. Lett., **72**, 3570 (1994).
2. K.M. Gambaryan, V.M. Aroutiounian and V.G. Harutyunyan. Infrared Phys. and Technol., **54**, 114 (2011).
3. K.M. Gambaryan. Nanoscale Res. Lett., **5**, 587 (2010).
4. V.M. Aroutiounian, K.M. Gambaryan and P.G. Soukassian. Surf. Sci., **604**, 1127 (2010).
5. H. Ihsiu and G.B. Stringfellow. Appl. Phys. Lett., **69**, 18 (1996).
6. S. Nakamura, M. Senoh, N. Iwasa and S. Nagahama. Jpn. J. Appl. Phys., **34**, L79 (1995).
7. S. Nakamura, M. Senoh, S. Nagahama, H. Iwasa, et al. Jpn. J. Appl. Phys., **35**, L74 (1996).
8. S. Strite and H. Morkoc. J. Vac. Sci. Technol., B **10**, 1237 (1992).
9. H.W. Kim, H.S. Kim, H.G. Na, J.C. Yang, et al. Chem. Eng. Journal **165**, 720 (2010).
10. J. Tersoff and R.M. Tromp. Phys. Rev. Lett., **70** (18), 2782 (1993).
11. M. Żenkiewicz. J. Achievements in Materials and Manufacturing Engineering **24**(1), 137 (2007).
12. M. Biehl, F. Much and C. Vey. Int. Series of Numerical Mathematics **149**, 41 (2005).
13. J. Shen, S. Johnston, S. Shang, T. Anderson. Journal of Crystal Growth **240**, 6 (2002).
14. J.G. Lozano, A.M. Sánchez, R. García, D. González. Appl. Phys. Lett., **87**, 263104 (2005).
15. Z. Bi, D. Lindgre, B.J. Johansson, et al. Phys. Stat. Solidi (c) **11**, 3 (2014).
16. W. Yang, J. Li, Y. Zhang, et al. Scientific Reports **4**, 5166 (2014).